

Engineering and Geological Aspects of the Wajid Sandstone, Najran-Khamis Mushayt Area, Southwestern Saudi Arabia, K.S.A.

A. K. Abd El-Aal

Geology Dept., Faculty of Science,
Al-Azhar University (Assuit Branch)
Assuit City, Egypt.
Ahmed_aka80@yahoo.com

I. A. EL Kharashy

Civil Engineering Dept.,
Najran University,
Najran City, K.S.A.

Abstract: *The Cambro-Ordovician sequences in Saudi Arabia are dominantly silicilastic, composed largely of medium to coarse-grained, cross-bedded sandstone of possible fluvial to deltaic origin. In the south and southwest, the Wajid Formation, considered the oldest formation in the region, overlies nonconformably on the Precambrian basement complex of igneous and metamorphic rocks. They form repeated fining-upward cycles, typical of deposition from braided streams. Petrographically, all samples of the Wajid Sandstone are of quartz arenite type, highly enriched in quartz, but poor in heavy minerals, feldspar and lithic fragments in the Najran and Khamis Mushayt at Al Gapha and Al Nakaa sections. The provenance and tectonic setting of the Wajid Sandstone have been assessed using integrated petrographic and geochemical studies. Petrographic analysis reveals that, mono- and poly-crystalline quartz grains and heavy minerals from metamorphic and igneous rocks of a craton interior setting were the dominant sources. Chemically, major and trace element concentrations in the rocks of the Wajid Sandstone indicate deposition in a passive continental margin setting. Petrographic and geochemical data suggest that the sediments were derived from metamorphic and igneous rocks forming the adjacent Precambrian basement rocks of the Arabian Shield, and were deposited on a passive continental margin. This study also includes the geotechnical properties of the Wajid Sandstone and its optimum utility for several uses at different locations which can be determined according to 1- physical properties {(grain size analysis (sieve and hydrometer analysis), permeability (hydraulic conductivity), moisture-density relation (compaction) test and porosity)} and 2- mechanical properties (direct shear test, unconfined compression (UC) test and consolidation test). Finally the sandstone can be used as construction materials (Mortar and Concrete), in road constructions as sub-base materials and as a source of silica.*

Keywords: *Wajid Sandstone; Petrographic analysis; geochemical studies; Provenance; geotechnical properties; optimum utility, Saudi Arabia*

1. INTRODUCTION

Two sections are selected to perform this study on the outcrops of the Wajid Sandstone (bounded by latitude 17° 30' to 20° 30' North and longitude 43° 30' to 46° 30' East) are found in the southwestern part of Saudi Arabia just west of the Rub' Al Khali Basin in the area between the Najran and Khamis Mushayt at Al Gapha and Al Nakaa sections (Fig. 1) which occupies most of south-central Arabia including Saudi Arabia, western Oman and the United Arab Emirates. The outcrops are continuous in the southern part of the Arabian Peninsula at the Wadi Ad-Dawasir on latitude 20° 30' N and extends to Najran at Latitude 17° 35' N and longitude 44° 45' E in the western end. The Wajid Sandstone extends over an area of 196 000 km² between Wadi Najran and Ash Sharawrah in the south, and Wadi Ad-Dawasir on its northern margin [1]. It also extends to Rub Al Khali Basin which is a frontier hydrocarbon province [2]; [3]. The Wajid Sandstone is a major water aquifer in

Saudi Arabia with a proven groundwater reserve of over 30, 000 million cubic meters [4]. The term 'Wajid Sandstone' was first used for the sandstone section exposed in the Gabal Al- Wajid, southwest Arabia [5]. This name was formally documented in published works [6]; [7]; [8]; & [9]. This rock unit is also defined by others [10]; [11] as the 'Wajid Formation'. The name Wajid Sandstone is ascribed to all sandstones in southern Saudi Arabia that occur directly above the Precambrian Arabian Shield and below Permian rocks [6]. The sandstone has been also described as of 'Nubian type' [7] because of its similarity to other similar sandstones exposed in North Africa, northern Saudi Arabia and Jordan [12].

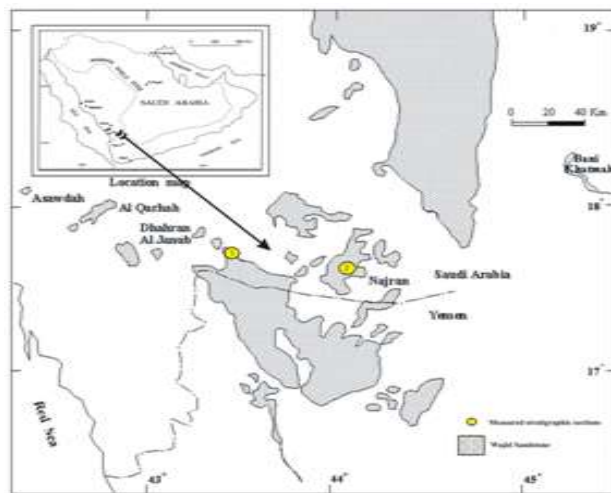


Figure1. Location map of the outcrops of the Wajid Sandstone in southwest Saudi Arabia (Simplified from [7])

2. SCOPE OF THE PRESENT STUDY

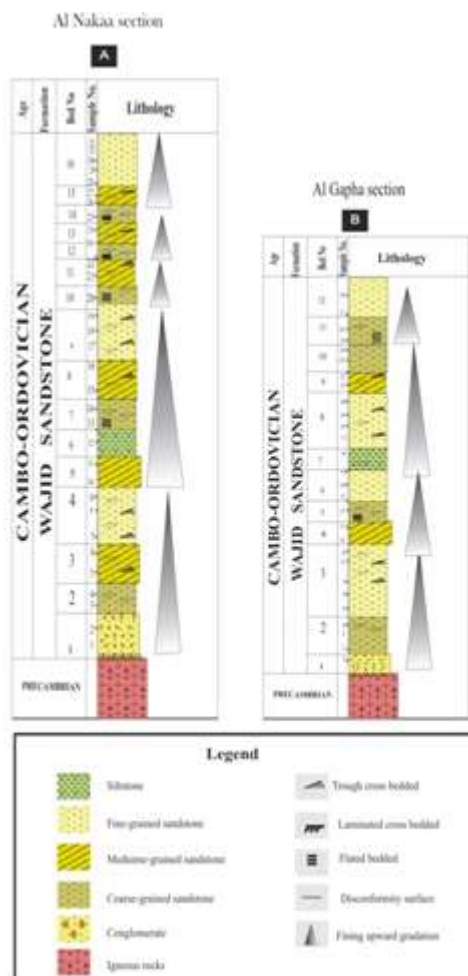


Figure2. Lithostratigraphic columnar sections of the Wajid Sandstone (see fig.1 for location of sections)

Several workers have worked on the Wajid Sandstone but no one has conducted detailed engineering characterization of each member of the Wajid Sandstone. A detailed investigation of

the sedimentology, lithofacies and engineering properties is required in order to have a better understanding of the Wajid Sandstone. The current study involves detailed field investigations, thin section petrography, measurements of physical and mechanical parameters such as porosity, permeability, sieve analysis, unconfined compressive strength and direct shear test and consolidation test, their statistical analysis, in order to throw more light on the economic importance on the Wajid Sandstone.

3. LITHOSTRATIGRAPHY

The Wajid Sandstone occurs as scattered outcrops in the area of study, in a series of hills and mesas. It rests unconformably on the peneplained basement rocks (mainly metamorphic and igneous rocks) of the Arabian Shield. The upper contact of the Wajid Sandstone does not occur in the study area, but in the extreme northeast at latitude it unconformably underlies the Permian Khuff Formation [13]. In the present work, two lithostratigraphic sections in the Wajid Sandstone, similar in their lithologic characters, were measured and described, these are between the Najran and Khamis Mushayt and termed Al Gapha and Al Nakaa sections (Fig. 2).

The age of Wajid Sandstone (Al Gapha and Al Nakaa sections), of probable Cambrian-Ordovician age, rest disconformably on crystalline rocks of the southern part of the Arabian shield. Scattered outcrops extend over an area about 450 km north-south and 300 km east-west. In the area of study, near the Yemen border, consists of fluvial sandstones and very minor siltstones and silty shales. The fluvial origin is demonstrated by the presence of fining-upward cycles, channels, trough cross bedding, and absence of all organic traces. The rocks exhibit variable colors of red, pale pink to pinkish brown and yellow. Most of the sandstones are friable to poorly cemented, while a few are cemented by iron oxides in the two studied sections . The lithologic sequence is characterized by repeated fining upward cycles, in which each cycle consists of a granule conglomerate at the base, followed upwards by coarse-to medium-grained sandstone, and topped by fine-grained sandstone and/or siltstone (See figure 2). The thickness of the cycles ranges from 4 to 10 m. Each cycle shows vertical variation in the primary sedimentary structures, with trough cross-bedded, pebbly coarse-grained sandstones at the base, followed upwards by planar cross-bedded, medium-grained sandstones, and terminated by flat-bedded to laminated fine

grained sandstones and siltstones in the upper part of the cycle. Fining-upward cycles and the vertical variation in the sedimentary structures has been interpreted as indicating deposition by a SW to N

The Wajid Sandstones vary from very fine- to very coarse-grained and from poorly- to very well-sorted with heterogeneous roundness of grains. Three architectural components, framework grains (av. 92.4% of the rock volume), and less frequently of feldspar, rock fragments

population is dominated by monocrystalline quartz, averaging 95.13 %, and mostly exhibit non-undulose (62%) to slightly undulose extinctions (36%). Monocrystalline quartz grains exhibit unit extinction and a few of them display undulose extinction. Heavy minerals form a minor constituent (less than 1%) of the sandstones and include rounded to well rounded grains of zircon, tourmaline, rutile, garnet, epidote and staurolite and opaque minerals. Polycrystalline grains are next in abundance (av. ~4.5%); almost all types described [14]. are observed in the Wajid sandstones. The most important are: 1) polycrystalline with two to five subcrystals and straight to slightly-curved intercrystalline boundaries; 2) those with elongated five or more crystals with sutured and crenulated intercrystalline subcrystal boundaries (Fig. 3 and 4A -B) Medium to coarse grained quartz arenite showing quartz overgrowth (Fig. 4-C-D). Feldspar occurs in the lower part of the succession at certain horizons, averaging 1.02% and is dominated by K feldspars such as microcline and less abundantly plagioclases, Table (1). The component of detrital grains is plotted on ternary diagram [15]. This indicates that most of the studied samples are of quartzarenite (Fig. 5).

5. GEOCHEMISTRY OF MAJOR ELEMENT

Major element chemistry has been used to discriminate the tectonic settings of sandstones since the studies carried out by [16]; [17]; [18], and has been commonly applied in more recent publications [16]. The major element chemistry of the Wajid Sandstones (Table 2) is discussed in terms of ternary plots and discrimination diagrams used to characterize tectonic setting proposed by [16]. These plots and diagrams show that the Wajid Sandstones were deposited in a passive continental margin tectonic setting (Fig. 5). The Wajid Sandstones are mainly composed of SiO₂, which ranges from 92.47 to 94.25 % (average = 93.62 %). CaO, Fe₂O₃ and Na₂O also present with averages of 1.02 %, 1.04 % and 1.95 %,

or NE-flowing river system all over the study area [8], [9].

4. PETROGRAPHIC INVESTIGATION

and heavy minerals (less than 3%). The quartz grains are rounded to subrounded and show point, straight to concavo-convex grain contacts.

The detrital mode is dominated by quartz, with variable amounts of lithic grains, minor feldspar, and accessory mica and heavy minerals. Quartz respectively (Table.2). Such geochemical data indicates that the sandstone is silica (Quartz) rich (Fig. 6).

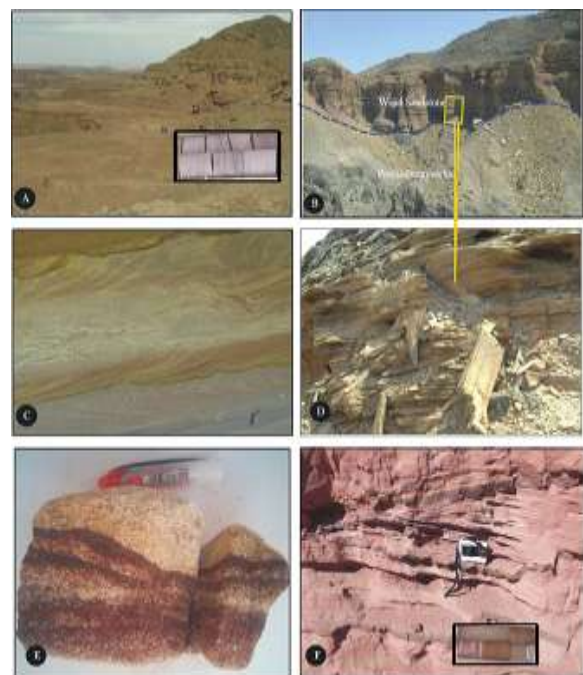


Figure 3.(A). General view of the Wajid Sandstone in Al Nakaa section – Corner photo showing the core sample used for UCS. (B) - The contact between the Precambrian rocks and Wajid Sandstone Al Gapha section. (C)- Field photograph showing the cross bedding sandstone in Al Gapha section. (D)- Field photograph showing thick bedded sandstone. (E): Sample showing the contact between the red and yellow sandstone. (F): Field photograph showing the thin bedded sandstone and the high concentration of iron oxides in the basal part of Wajid Sandstone at Al Gapha section- Corner photo showing the core sample used for UCS.

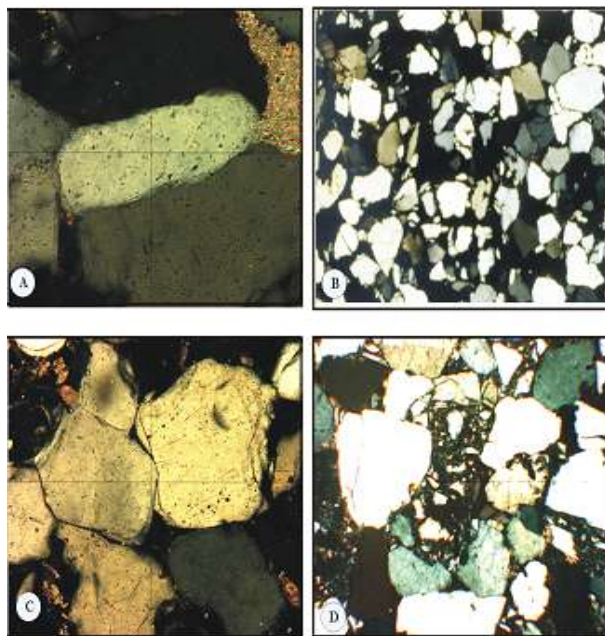


Figure 4A. Photomicrograph showing quartz arenite consisting mainly of monocrystalline quartz crystals with straight to slightly curved intercrystal boundaries (B) Medium to coarse grain quartz arenite with quartz content exceeding 95%; (C) polycrystalline quartz grain showing quartz overgrowth; (D) polycrystalline quartz grain and Sedimentary rock fragments. (All photomicrograph with 20 X)

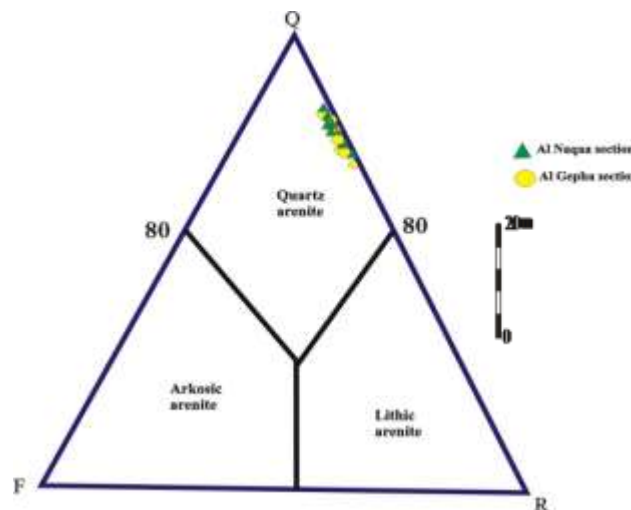


Figure5. Ternary plot of detrital components of the Wajid Sandstone on the tectonic provenance discrimination diagram [15]. Q is the total quartz, F is the feldspar, L is the total rock fragments.

6. GEOTECHNICAL FEATURES (PHYSO-MECHANICAL PROPERTIES)

Construction materials in general are important components of infrastructure, such as roads, buildings, airports, etc. Sandstone is one of the most important raw and construction materials.

The last years, the demand for sandstone, as construction and structure materials, in KSA, has

markedly increased. It becomes therefore national need to satisfy the requirements of several industrial uses. Optimum utility of sandstone for several uses at different locations can be determined according to the main following parameters:

1- physical properties (grain size analysis (Sieve and Hydrometer analysis), permeability "Hydraulic conductivity", moisture-density relation "Compaction" test and porosity).

- mechanical properties (direct shear test, unconfined compression "UC" test and consolidation test)

A- Grain Size Analysis (Sieve and Hydrometer Analysis)

This test is performed to determine the percentage of different grain sizes contained within a soil. The mechanical or sieve analysis is performed to determine the distribution of the coarser, larger-sized particles, and the hydrometer method is used to determine the distribution of the finer particles. The distribution of different grain sizes affects the engineering properties of soil. Grain size analysis provides the grain size distribution, and it is required in classifying the soil (Fig. 7).

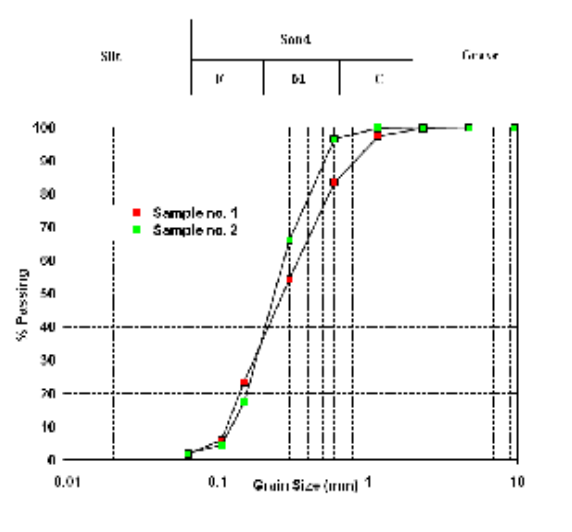


Figure7. Sieve analysis test of two selected sample along the study area (sample 1 for Al naka section and sample 2 for Al Gapha section)

B- Permeability (Hydraulic Conductivity) Test Constant Head Method

Permeability (or hydraulic conductivity) refers to the ease with which water can flow through a soil. This property is necessary for the calculation of seepage through earth dams or under sheet pile walls, the calculation of the seepage rate from waste storage facilities (landfills, ponds, etc.), and

the calculation of the rate of settlement of clayey soil deposits.

$$Kt = Q/At$$

Where:

KT = coefficient of permeability at temperature T, cm/sec.

L = length of specimen in centimeters.

t = time for discharge in seconds.

Q = volume of discharge in cm³ (assume 1 mL = 1 cm³).

A = cross-sectional area of permeameter.

Table1. Modal analysis data of the selected sandstone samples in the study area

Location	Sample No	Mono Qtz%	Non undulose Qtz%	Undulose Qtz%	Poly Qtz%	Total Qtz%	Feldspar%	Rock fragments%
Al Nakaa	1	93.9	62.3	31.60	5	192.80	1.25	0.54
	2	93.39	63.25	30.14	4.25	191.03	1.65	58
	3	96.31	64.21	32.11	3.25	195.87	0.98	1.24
	4	95.39	63.85	31.54	4.98	195.76	0.79	1.25
	5	95.55	62.35	33.2	4.75	195.85	0.83	1.02
	6	96.29	61.25	35.04	4.62	197.22	1.05	0.25
	7	94.24	62.84	31.40	4.15	192.63	1.06	0.98
	Ava	95.10	62.95	32.15	4.45	194.67	1.032	8.01
Al Gapha	1	94.95	62.41	32.54	3.65	193.55	0.85	1.02
	2	95.9	63.25	32.65	2.54	194.34	0.65	0.45
	3	98.12	63.87	34.25	4.36	200.60	0.98	0.92
	4	94.03	61.52	32.51	3.98	192.04	0.74	0.33
	5	92.38	62.37	30.01	4.15	188.91	1.02	0.54
	6	96.02	63.51	32.51	2.58	194.62	1.65	29
	7	94.54	61.29	33.25	2.69	191.77	0.74	0.74
	Ava	95.13	62.60	32.53	3.42	193.69	0.94	4.71

Table2. Major oxide values of the selected sandstone samples in the study area.

Location	Sample No	SiO ₂ %	Al ₂ O ₃ %	Fe ₂ O ₃ %	MgO%	CaO%	Na ₂ O%
Al Nakaa	1	92.5	3.21	0.21	0.12	2.21	1.25
	2	93.2	2.54	0.65	0.31	2.35	2.21
	3	92.6	4.21	0.28	0.04	1.05	2.36
	4	93.2	3.98	0.78	0.05	1.25	2.85
	5	94.2	4.47	1.25	0.01	1.05	3.21
	6	93.2	2.95	1.54	0.03	1.06	2.47
	7	92.5	3.47	1.02	0.01	2.14	1.01
	8	92.1	3.87	0.98	0.03	1.06	0.21
Ava	92.9	3.59	0.84	0.075	1.52	1.95	
Al Gapha	1	92.7	4.01	0.29	0.03	2.01	0.36
	2	92.7	2.87	0.98	0.01	0.12	0.29
	3	92.4	2.58	1.06	0.02	0.098	0.85
	4	92.7	3.98	1.09	0.03	0.24	0.74
	5	92.4	4.6	1.65	0.01	1.03	1.25
	6	93.4	4.02	1.41	0.02	1.09	2.12

	7	94.7	3.21	0.65	0.01	1.08	2.15
	Ava	93.0	3.53	1.02	0.02	0.81	1.11

h = hydraulic head difference across length.

A = cross-sectional area of permeameter.

Localities	Constant Head, h (cm)	Elapsed Time, t (seconds)	Outflow Volume, Q (cm ³)	Water Temp., T (°C)	KT cm/sec	K20 cm/sec
Al Nakaa	30	84	750	22	0.157	0.149
	50	55	750	22	0.144	0.137
	60	48	750	22	0.137	0.130
	70	38	750	22	0.149	0.142
	K20					0.139 cm/sec
Al Gapha	30	85	750	22	0.156	0.147
	50	60	750	22	0.142	0.135
	60	46	750	22	0.135	0.128
	70	36	750	22	0.146	0.138
	K20					0.137 cm/sec

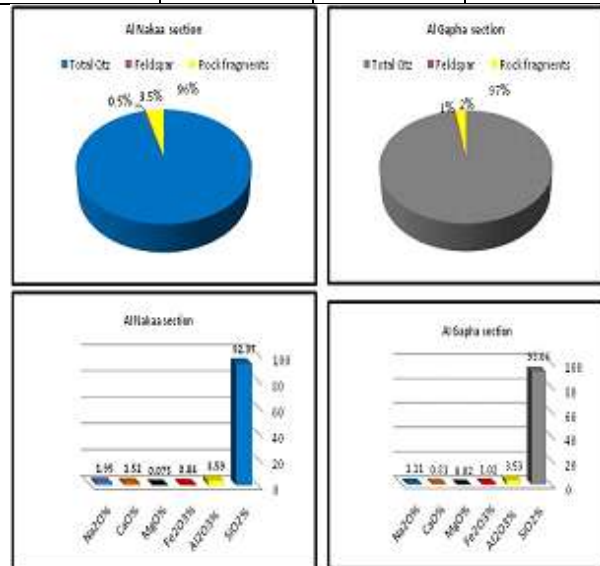


Figure 6. Pie chart showing the mean components and major element of sandstone sample at the two localities of the study area.

Table 3. Values of effective depth based on hydrometer and sedimentation cylinder of specific sizes.

Commonly the Permeability ranging from 0.139 to 0.137 Cm/Sec over all the studied area (Table No.4)

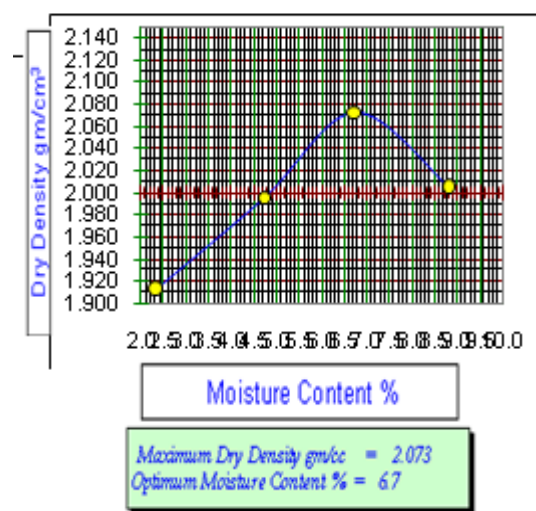
Table 4. Permeability values of the selected sandstone samples in the study area

Time (min)	Hydrometer Reading	Effective Depth (L)	Particle Diameter (mm)	% finer (of tested sample)	% finer (of total sample)
0.5	1.0285	8.76	0.0519	88.4	84.1
1	1.028	8.89	0.0370	86.5	82.4
2	1.027	9.16	0.0265	82.9	79.0
4	1.026	9.42	0.0190	79.3	75.6
8	1.024	9.95	0.0138	72.1	68.7
15	1.0225	10.35	0.0103	66.7	63.5
30	1.0205	10.88	0.0075	59.5	56.7

60	1.018	11.54	0.0054	50.5	48.1
120	1.016	12.07	0.0039	43.3	41.2
1440	1.008	14.19	0.0012	14.4	13.7
2880	1.006	14.73	0.0009	7.2	6.9
4320	1.005	14.99	0.0007	3.6	3.4
5760	1.005	14.99	0.0006	3.6	3.4

C- Moisture-Density Relation (Compaction) Test.

Mechanical compaction is one of the most common and cost effective means of stabilizing soils. An extremely important task of geotechnical engineers is the performance and analysis of field control tests to assure that compacted fills are meeting the prescribed design specifications. Design specifications usually state the required density (as a percentage of the “maximum” density measured in a standard laboratory test), and the water content. In general, most engineering properties, such as the strength, stiffness, resistance to shrinkage, and imperviousness of the soil, will improve by increasing the soil density. The maximum density ranging from 2.011 to 2.073 gm/cc, (Fig. 7).



E- Direct Shear Test

This test is performed to determine the consolidated-drained shear strength of a sandy to silty soil. The shear strength is one of the most important engineering properties of a soil, because it is required whenever a structure is dependent on the soil’s shearing resistance [19]. The shear strength is needed for engineering situations such as determining the stability of slopes or cuts,

Figure7. Maximum dry density of sandstone sample in El-Naqaa area.

D- Porosity

The porosity is defined as the ratio of the volume of voids expressed as a percentage of the total (bulk)

volume of a rock, including the solid and void components. In general, porosity is the property of solid to have free spaces, or pores, between individual particles not filled by the structural materials. Quantitatively, porosity is defined by the volume of pores per unit volume of a material.

The porosity (N %) by polished surface area were calculated as follows [17].

$$V_P = W_2 \cdot W_1$$

$$N = V_P / V_b * 100\%$$

W_1 = Weight of the dry sample, gm.

W_2 = weight of specimen after immersion, gm.

V_b = Volume of the bulk sample, cm^3 .

V_P = Volume of the pore space in the sample, cm^3 .

N= Total porosity of the rock %.

The results of porosity of the studied samples of all locations are given in Table (5).

finding the bearing capacity for foundations, and calculating the pressure exerted by a soil on a retaining wall. The direct shear test is one of the oldest strength tests for soils. In this laboratory, a direct shear device will be used to determine the shear strength of a cohesionless soil (i.e. angle of internal friction (f)).

E- Direct Shear Test

This test is performed to determine the consolidated-drained shear strength of a sandy to silty soil. The shear strength is one of the most important engineering properties of a soil, because it is required whenever a structure is dependent on the soil's shearing resistance [19]. The shear strength is needed for engineering situations such as determining the stability of slopes or cuts, finding the bearing capacity for foundations, and calculating the pressure exerted by a soil on a retaining wall. The direct shear test is one of the oldest strength tests for soils. In this laboratory, a direct shear device will be used to determine the shear strength of a cohesionless soil (i.e. angle of internal friction (f)).

In terms of effective stresses, the effective shear strength, τ' , can be re-written as follows:

$$\tau' = c' + (\sigma_n - u) \tan \phi' = c' + \sigma' \tan \phi'$$

Where u is the pore water pressure, c' is the effective cohesion, σ' is the effective normal

Table6. Horizontal displacement and horizontal shear force reading.

Horizontal Dial Reading (0.001 in)	Horizontal Displacement (in)	Load dial Reading	Horizontal Shear Force (lb)	Shear Stress (psi)
0	0	0	0	0
1	0.001	16	8.706	1.801
5	0.005	22	10.488	2.170
10	0.01	27	11.972	2.478
15	0.015	31	13.16	2.723
21	0.021	34	14.052	2.908
28	0.028	36	14.646	3.031
34	0.034	41	16.131	3.338
39	0.039	41.5	16.279	3.37
42	0.042	43	16.725	3.461
51	0.051	45	17.319	3.584
61	0.061	47	17.913	3.707
68	0.068	50	18.804	3.891
74	0.074	54	19.99	4.13
82	0.082	56	20.586	4.26
88	0.088	58	21.18	4.383
94	0.094	61	22.071	4.568
101.5	0.1015	63	22.665	4.690
109	0.109	67	23.85	4.937
115	0.115	72	25.337	5.244
122	0.122	75	26.228	5.428
128	0.128	78	27.119	5.612
133	0.133	82	28.307	5.858
138	0.138	83	28.605	5.92
142	0.142	83	28.60	5.92

Stress, and ϕ' is the effective friction angle. (Fig. 8).

In this laboratory, a direct shear device will be used to determine the shear strength of a cohesionless soil (i.e. angle of internal friction (f)) (Fig.10-A). From the plot of the shear stress versus the horizontal displacement, the maximum shear stress is obtained for a specific vertical confining stress. After the experiment is run several times for various vertical-confining stresses, a plot of the maximum shear stresses versus the vertical (normal) confining stresses for each of the tests is produced. From the plot, a straight-line approximation of the Mohr-Coulomb failure envelope curve can be drawn, f may be determined, and, for cohesionless soils ($c = 0$), the shear strength can be computed from the following equation: $S = s \tan f$. The angle of internal friction (f) of Waljid Sandstone is between 45° to 48° Table (6).

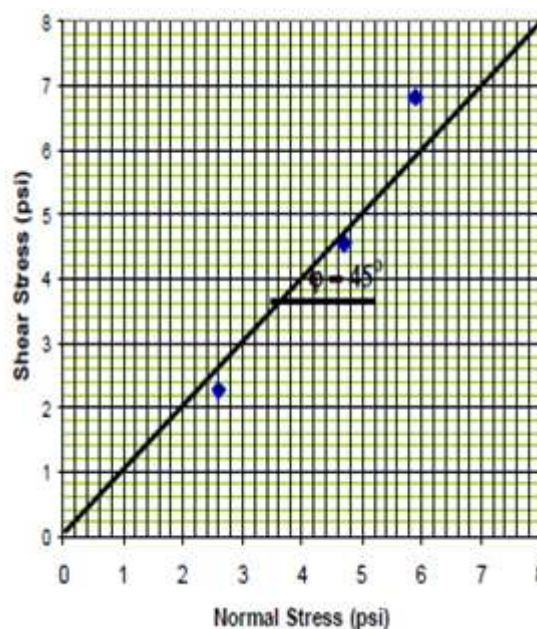


Figure8. Relationship between the shear stress and normal stress.

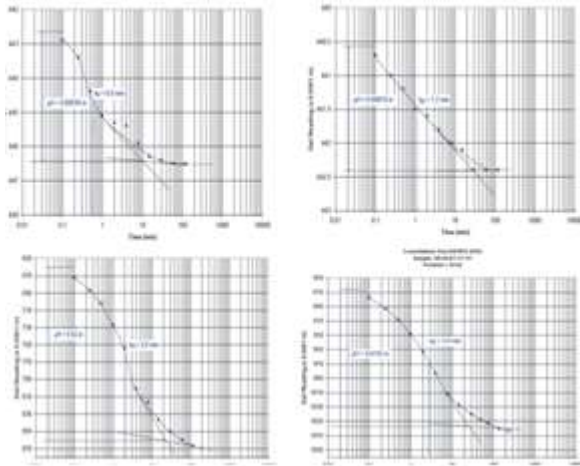


Figure9. Dial reading Vs time at different pressure loads.

F- Consolidation Test

This test is performed to determine the magnitude and rate of volume decrease that a laterally confined soil specimen undergoes when subjected to different vertical pressures. From the measured **Table7. Analysis of consolidation test data**

data, the consolidation curve (pressure-void ratio relationship) can be plotted. This data is useful in determining the compression index, the recompression index and the preconsolidation pressure (or maximum past pressure) of the soil. In addition, the data obtained can also be used to determine the coefficient of consolidation and the coefficient of secondary compression of the soil (ASTM 1958).

Final Results:

Compression Index (C_c) = 0.11.

Recompression Index (C_r) = 0.013.

Preconsolidation pressure (P_c) or Maximum past pressure (σ_{vmax}) = 3.5 tsf.

Coefficient of consolidation (C_v) = 1.54×10^{-2} to 9.01×10^{-3} in²/min (depends on the pressure) Table no. 7 and (Fig. 9 and Fig.10-B).

Pressure (tsf)	Time for 50% consolidation t_{50} (min)	D_0 (from graph)	D_{100} (from graph)	$D_{50} = (D_1 + D_{100}) * 0.5$	$H_s = D_{50} * 0.001$	ΔH (from graph)	$\Sigma \Delta H$	H^*	H_d^{**}	Coefficient of consolidation C_v (in ² /min) ^{***}	H_v	e^{***}
0								1.06299				
0.5	10	8	159	83.5	0.00835	0.0153	0.0153	1.04769	0.5293	5.45E-03	0.34	0.48
1	11.5	173	254	213.5	0.02135	0.008	0.0233	1.03969	0.52518	4.72E-03	0.33	0.47
2	30	254	301	277.5	0.02775	0.0048	0.0281	1.03489	0.52438	1.81E-03	0.33	0.47
4	33	310	362	336	0.03360	0.0156	0.0437	1.01929	0.51805	1.60E-02	0.31	0.44
2	1.9	496	492.5	494.25	0.04943	0.0004	0.04335	1.01964	0.52218	2.83E-02	0.31	0.44
1	3.5	493	472.5	482.5	0.04825	0.002	0.04132	1.02167	0.52290	1.54E-02	0.32	0.45
0.5	6	472	442	457	0.04570	0.0029	0.03842	1.02457	0.52371	9.01E-03	0.32	0.45
1	1.2	441	442.4	441.5	0.04415	0.0002	0.0386	1.02439	0.52323	4.49E-02	0.32	0.45
2	0.6	443	445.5	444.55	0.04446	0.0004	0.03898	1.02401	0.52312	8.98E-02	0.32	0.45
4	2.4	446	489	467.5	0.04675	0.0043	0.04328	1.01971	0.52154	2.23E-02	0.31	0.44
8	3	504	650	577	0.05770	0.0143	0.05758	1.00541	0.51713	1.76E-02	0.30	0.42
16	2	660	861	760.5	0.07605	0.02	0.07758	0.98541	0.51172	2.58E-02	0.28	0.40
32	3	869	1060	964.5	0.09645	0.0192	0.09678	0.9662	0.50722	1.69E-02	0.26	0.37

							1			
								55	54	27.09
							Ava.	27.09		

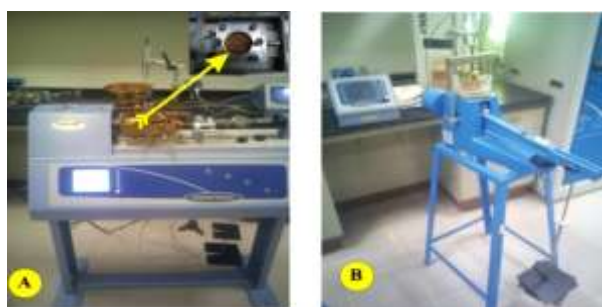


Figure10. (A)-Shear box test equipment and (B) Consolidation Test equipment.

G- Unconfined Compression (Uc) Test

The primary purpose of this test is to determine the unconfined compressive strength, which is then used to calculate the unconsolidated undrained shear strength of the clay under unconfined conditions. According to the ASTM standard, the unconfined compressive strength (q_u) is defined as the compressive stress at which an unconfined cylindrical specimen of soil will fail in a simple compression test. In addition, in this test method, the unconfined compressive strength is taken as the maximum load attained per unit area, or the load per unit area at 15% axial strain, whichever occurs first during the performance of a test. For soils, the undrained shear strength (s_u) is necessary for the determination of the bearing capacity of foundations, dams, etc (ASTM 1958). The undrained shear strength (s_u) of sand is commonly determined from an unconfined compression test Table no. 8.

Table8. The UCS results of sandstone at different localities.

Localities	Test No.	Test Result (kN)	Diameter (mm)	UCS (MPa)
Al Nakaa		67.8	54	29.6
		70.00	54	30.56
		58.00	54	25.33
		59.00	54	25.76
	Ava.	27.81		
Al Gapha		55	54	24.03
		61	54	26.65
		65	54	28.40
		67	54	29.27

7. CONCLUSION

The Wajid Sandstone, of probable Cambro-Ordovician age. rests disconformably on crystalline rocks of the southern part of the Arabian shield. Scattered outcrops extend over an area about 450 km north-south and 300 km east-west. The southern part of the formation, near the Yemen border, consists of fluvial sandstones and very minor siltstones and silty shales. The fluvial origin is demonstrated by the presence of fining-upward cycles, channels, trough cross bedding, and absence of all organic traces. The northern part of the outcrop area consists of internally homogeneous, tabular cross-bedded, horizontally bedded sandstones apparently formed in a shallow marine environment.

Microscopic investigation of selected samples of the Wajid Sandstone showed that the sandstones are chiefly vary from very fine- to very coarse-grained and from poorly- to very well-sorted with heterogeneous roundness of grains. Three architectural components, framework grains (av. 92.4% of the rock volume), and less frequently of feldspar, rock fragments and heavy minerals (less than 3%). The quartz grains are rounded to subrounded and show point, straight to concavo-convex grain contacts. The detrital mode is dominated by quartz, with variable amounts of lithic grains, minor feldspar, and accessory mica and heavy minerals. Quartz population is dominated by monocrystalline quartz , averaging 95.13 %, and mostly exhibit nonundulose (62%) to slightly undulose extinctions (36%). Monocrystalline quartz grains exhibit unit extinction and a few of them display undulose extinction. Heavy minerals form a minor constituent (less than 1%) of the sandstones and include rounded to well rounded grains of zircon, tourmaline, rutile, garnet, epidote and staurolite and opaque minerals. Polycrystalline grains are next in abundance (av. ~4.5%).

Petrographic data (framework mineralogy, quartz types and heavy minerals) obtained from the study of the Wajid Sandstone suggest that metamorphic and plutonic igneous rocks in a cratonic interior were the most important source rocks for the Wajid Sandstone. These source rocks were most probably the basement rocks of the adjacent Arabian Shield.

The Wajid Sandstones are mainly composed of SiO₂, which ranges from 92.47 to 94.25 % (average = 93.62 %). CaO, Fe₂O₃ and Na²O also present with averages of 1.02 %, 1.04 % and 1.95 %, respectively (Table. 4.4). Such geochemical data indicates that the sandstone is silica (Quartz) rich. Therefore, the petrographic and geochemical data suggested that the Wajid Sandstone was derived from the Precambrian basement rocks of the southeastern margin of the Arabian Shield, and was deposited in a passive margin setting after the stabilization of the Arabian Shield following the Late Precambrian Pan- African Orogeny. Optimum utility of sandstone for several uses at different locations can be determined according to the main following parameters:

1- Physical properties (grain size analysis (sieve and hydrometer analysis) which showing that, the Wajid Sandstone is commonly medium to coarse graine, permeability (hydraulic conductivity) Permeability ranging from 0.139 to 0137 Cm/ Sec over all the studied area, moisture-density relation (compaction) test ,), the maximum density ranging from 2.011 to 2.041 gm/cc and porosity. The results of porosity of the studied samples ranging from 16.62 to 18.5 %.

2- Mechanical properties (direct shear test. The angle of internal friction (f) of Wajid Sandstone is between 45 to 48o , unconfined compression (ucs) ranging from 27.09 to 27.81 MPa and consolidation test). Finally Wajid Sandstone can be used as construction materials (Mortar and Concrete), in road constructions as sub-base materials and as a source of silica for different chemical and industrial uses.

ACKNOWLEDGEMENTS

The authors wish to thank the Najran University, faculty of Engineering, Saudi Arabia for providing necessary logistic and technical support to carry out the research. Thanks also go to Prof. Dr. M. A. Khalifa Professor of sedimentary rocks, Faculty of Science, Geology Department, El Menoufiya University, for his critical review of the original manuscript and constructive suggestions for upgrading the clarity of the manuscript.

REFERENCES

[1] Brown, G.F., D.L. Schmidt and A.C. Huffman. 1989. Geology of the Arabian Peninsula; Shield area of western Saudi Arabia. US Geological Survey Professional Paper 560A, 188 p.

[2] Amireh, B.S. 1991. Mineral composition of the Cambrian-Cretaceous Nubian series of

Jordan: provenance, tectonic setting and climatological implications. *Sedimentary Geology*, V. 71, Pp. 99-119.

[3] Evans, D.S, R.B. Lathon, M. Senalp and T.C. Connally. 1991. Stratigraphy of the Wajid sandstone of southwestern Saudi Arabia. *Proceedings of the Society of Petroleum Engineers Middle East Oil Show, Bahrain*, 16-19 November, 1991, SPE paper 21449, Pp. 947-957.

[4] Al Alawi, M. and Abdulrazzak, M. 1994): Water in the Arabian Peninsula: Problems and Perspectives, in P. Rogers and P. Lydon (eds.), *Water in the Arab World: Perspectives and Progress*.

[5] Jackson, R.O., Bogue, R.G., Brown, G.F., Gierhart, R.D., 1963. Geologic map of the southern Najd quadrangle, Saudi Arabia. Saudi Arabian Deputy Ministry for Mineral Resources, Map I-211 A.

[6] Powers, R.W. Ramirez, L.F., Redmond, C.D., Elberg, E.L., 1966. Geology of the Arabian Peninsula: sedimentary geology of Saudi Arabia. US Geological Survey Professional Paper 560D.

[7] Hardley, D.G., Schmidt, D.L., 1975. Non-glacial Origin for Conglomerate Beds in the Wajid Sandstone of Saudi Arabia. Directorate General of Mineral Resources, United States of America, Geological Survey, Saudi Arabia Report, 174 pp.

[8] Dabbagh, M.E., Rogers, J.J., 1983. Depositional environments and tectonic significance of the Wajid Sandstone of southern Saudi Arabia. *Journal of African Earth Sciences* v. 1, Pp. 47–57.

[9] Moshrif, M.A., El-Hitt, A., 1989. Lithofacies and petrography of Wajid Sandstone (Cambrian–Ordovician) Saudi Arabia. *Journal of African Earth Sciences* V. 9, Pp. 401–412.

[10] Pallister, J.S., 1982. Reconnaissance geology of Jabal Al-Ilman quadrangle, sheet 18/44A. Saudi Arabian Deputy Ministry for Mineral Resources, open file report USGS-OF- V. 02. Pp. 90, 61.

[11] Kellogg, K.S., Fourniguet, J., Janjou, J., Minoux, L., 1986. Geologic map of the Wadi Tathlith quadrangle, Sheet-20G, Saudi Arabian Deputy Ministry for Mineral Resources, Map GM-103 A, Scale 1:250,000.

[12] Beydoun, Z.R., 1988. *The Middle East: Regional Geology and Petroleum Resources*. Scientific Press, UK. 291p.

[13] Khalifa, M.A. (2010): Revised lithostratigraphic classification of Upper

- Permian–Lower Triassic strata in Saudi-Arabia: regional correlation and depositional history. *Paläontologie, Stratigraphie, Fazies* (18), Freiburger Forschungshefte, C 536: Pp 157–181; Freiberg.
- [14] Blatt, H. (1982): *Sedimentary Petrology*, W. H. Freeman. San Francisco, California, p. 564.
- [15] Dickinson, W.R., Beard, L.S., Brakenridge, G.R., Erjavec, J.L., Ferguson, R.C., Inman, K.F., Knepp, R.A., Lindberg, F.A., Ryberg, P.T., 1983. Provenance of North American Phanerozoic sandstones in relation to tectonic setting. *Geological Society of American Bulletin*. V. 94, Pp.222–235.
- [16] Schwab, F.L., 1975. Framework mineralogy and chemical composition of continental margin-type sandstone. *Geology* V. 3, Pp. 487-490.
- [17] Bhatia, M.R., 1983. Plate tectonics and geochemical composition of sandstones. *Journal of Geology* V. 91, Pp 611–627.
- [18] Zimmermann, U., Bahlburg, H., 2003. Provenance analysis and tectonic setting of the Ordovician clastic deposits in the southern Puna Basin, NW Argentina. *Sedimentology* V. 50, Pp. 1079–1104.
- [19] ASTM, 1958. *Standards of Building Stones*. Part 5, Pp. 9-3